Journal of Power Sources 243 (2013) 323–327

Contents lists available at SciVerse ScienceDirect

Journal of Power Sources

journal homepage: www.elsevier.com/locate/jpowsour

Short communication

Charge/discharge performances of glyme–lithium salt equimolar complex electrolyte for lithium secondary batteries

Shiro Seki [a,*], Nobuyuki Serizawa [a], Katsuhito Takei [a], Kaoru Dokko [b], Masayoshi Watanabe [b]

[a] Materials Science Research Laboratory, Central Research Institute of Electric Power Industry (CRIEPI), 2-11-1, Iwado-kita, Komae, Tokyo 201-8511, Japan
[b] Department of Chemistry and Biotechnology, Yokohama National University, 79-5, Tokiwadai, Hodogaya-ku, Yokohama, Kanagawa 240-8501, Japan

HIGHLIGHTS

- A glyme–Li salt equimolar complex exhibited the high stability with the Li metal.
- Favorable charge/discharge over 600 cycles was achieved for [$LiFePO_4$|Li] cell.
- [$LiNi_{1/3}Mn_{1/3}Co_{1/3}O_2$|Li] cell showed stable charge/discharge up to 400 cycles.

ARTICLE INFO

Article history:
Received 26 April 2013
Received in revised form
22 May 2013
Accepted 2 June 2013
Available online 18 June 2013

Keywords:
Glyme
Lithium salt
Safety electrolyte
Long cycle life
Charge/discharge

ABSTRACT

The electrochemical and battery performances of a CH_3–O–$(C_2H_4O)_3$–CH_3/$LiN(SO_2CF_3)_2$ 1:1 equimolar complex electrolyte were evaluated using [Li metal|Li metal], [$LiFePO_4$|Li metal], and [$LiNi_{1/3}Mn_{1/3}Co_{1/3}O_2$|Li metal] cells. A relatively favorable surface was formed at the Li metal/electrolyte interface revealed by observation of the storage time dependence of the electrochemical impedance spectroscopy. A 3V-class [$LiFePO_4$|Li metal] cell exhibited favorable capacity retention with little degradation after 600 cycles (2.5–4.0 V). A 4V-class [$LiNi_{1/3}Mn_{1/3}Co_{1/3}O_2$|Li metal] cell also exhibited good capacity retention of approximately 60% of the initial discharge capacity after 400 cycles (2.7–4.2 V), while the capacity retention decreased markedly upon increasing the upper charge cutoff voltage above 4.4 V.

1. Introduction

The competition to increase the performance and reduce the cost of lithium-ion batteries is growing intense, because of the advances in consumer electronic devices and transportation [1]. Safety is a key issue for lithium-ion batteries with high energy density (per volume and weight) as well as battery size. In order to improve the safety of electrolytes, organic solids (polymers) [2–4], inorganic solids (ceramics) [5,6], and room-temperature ionic liquids [7–12] have been proposed as new electrolytes for safe electrolyte materials to avoid severe accidents. Recently, 1:1 equimolar complex electrolytes with low-molecular-weight ether (glyme) and lithium salts have been reported to exhibit high thermal stability due to the strong interactions between the oxygen in ether and the lithium cations. Such electrolyte systems gather attentions to be used in highly safe lithium secondary batteries [13,14]. The main feature of these electrolyte materials is the similarity to room-temperature ionic liquids with strongly solvated lithium ions and glyme molecules (such as cations) and dissociated anions. Moreover, such electrolyte systems have no free ether units with the rigid complexes between Li and O, and exhibit high oxidative stability (with oxidized positive electrode active materials) [15,16] and reasonably low solubility (with sulfur-containing positive electrode active materials) [17]. We also reported the operation of lithium-ion batteries with positive ($LiFePO_4$) and negative (graphite) electrodes using $N(SO_2F)_2$ anion [18]. In order to practically use glyme–lithium salt complex electrolytes as new battery electrolyte materials in the future, detailed electrochemical evaluations and long cycle life tests of the cells using well-known

* Corresponding author. Tel.: +81 3 3480 2111; fax: +81 3 3480 3401.
E-mail address: s-seki@criepi.denken.or.jp (S. Seki).

0378-7753
http://dx.doi.org/10.1016/j.jpowsour.2013.06.005

positive electrodes and a lithium metal electrode are necessary. In this study, to investigate the charge/discharge performances (capacity retention, Coulombic efficiency) and the operation voltage using glyme–lithium salt equimolar mixture as an electrolyte, we used 3V-class $LiFePO_4$ and 4V-class $LiNi_{1/3}Mn_{1/3}Co_{1/3}O_2$ positive electrodes and carried out long cycle life tests of reaching up to 600 ($LiFePO_4$) and 400 ($LiNi_{1/3}Mn_{1/3}Co_{1/3}O_2$) charge–discharge cycles, and we will discuss its performance as the electrolyte materials for lithium secondary batteries.

2. Experimental

2.1. Samples

Distilled and dried triethylene glycol dimethyl ether (triglyme, G3, Kishida Chemical Co., Ltd.) and lithium bis(trifluoromethanesulfonyl) amide ($LiN(SO_2CF_3)_2$, LiTFSA, Kishida Chemical Co., Ltd.) were used as the solvent and lithium species, respectively. These materials were stored in a dry-argon-filled glovebox. Equimolar amounts of G3 and LiTFSA were weighed and mixed in a sample bottle, which allow us to obtain a homogeneous liquid electrolyte.

2.2. Electrochemical characteristics of metallic lithium electrode/G3–LiTFSA electrolyte

The storage time dependence of the G3–LiTFSA electrolyte/metallic lithium interfacial resistance ($R_{lithium}$) in [lithium metal (Honjo Metal, thickness: 300 μm)|G3–LiTFSA electrolyte + separator|lithium metal] symmetrical cells (2032-type coin cells) was investigated by the AC impedance method using an electrochemical measurement system (Bio-Logic, VMP3, 200 kHz–50 mHz, applied voltage: 10 mV) at 40 °C with measurements at 5 h intervals. The temperature dependence of $R_{lithium}$ was measured at temperatures between 0 °C and 80 °C with heating using the above-mentioned cell. The cell was thermally equilibrated at each temperature for at least 90 min prior to measurements.

2.3. Fabrication and electrochemical evaluation of lithium secondary batteries

Lithium secondary battery characteristics were investigated using [positive electrode ($LiFePO_4$, $LiNi_{1/3}Mn_{1/3}Co_{1/3}O_2$)|G3–LiTFSA electrolyte + separator|lithium metal negative electrode] cells. The positive electrode sheet was composed of $LiFePO_4$ or $LiNi_{1/3}Mn_{1/3}Co_{1/3}O_2$ (85 wt.%) as the active material, acetylene black (3 wt.%, Denka) and vapor grown carbon fiber (3 wt.%, Showa Denko) as an electrically conductive additive, and PVdF (9 wt.%, Kureha Chemical) as a binder polymer (positive active electrode material weight: 2–3 mg cm^{-2}). These constitutive materials were thoroughly stirred together in a homogenizer with *N*-methylpyrrolidone (NMP). The obtained positive electrode paste was uniformly applied onto an aluminum current collector using an automatic applicator. After drying the applied paste, the positive electrode sheets were compressed using a roll-press machine to increase packing density and improve electrical conductivity (pressed thickness: *ca.* 20 μm). The positive electrode sheet (ϕ16), polypropylene-based separator (ϕ19), G3–LiTFSA electrolyte, and lithium metal negative electrode (ϕ16) were encapsulated into 2032-type coin cells. To ensure complete penetration of the electrolyte into the high-density pressed positive electrode sheet, the prepared cells were aged at 60 °C for more than 18 h. Then, charge/discharge tests were performed on the cells at 2.5–4.0 V ($LiFePO_4$), and 2.7–4.2, 2.7–4.4, and 2.7–4.6 V ($LiNi_{1/3}Mn_{1/3}Co_{1/3}O_2$) with a current of *ca.* C/8 under a constant current charge and a constant current discharge using a charge/discharge unit (HJ-SM8, Hokuto Denko). All charge/discharge tests were performed at 30 °C.

3. Results and discussion

3.1. Stability of G3–LiTFSA electrolyte/lithium metal electrode interface

To investigate the electrochemical stability of the G3–LiTFSA electrolyte on the reduction (anodic) side, the interfacial behavior at the electrolyte/lithium metal electrode was examined under static condition. Fig. 1(a) shows the storage time dependence of the AC impedance spectrum of the [lithium metal|G3–LiTFSA electrolyte|lithium metal] symmetrical cell measured at 40 °C. Because the symmetrical cell is bipolar, impedance response consists of the G3–LiTFSA electrolyte bulk resistance (R_{bulk}) and the G3–LiTFSA electrolyte/lithium metal electrode interfacial resistance ($R_{lithium}$). $R_{lithium}$ contains the components of the charge-transfer resistance and the solid electrolyte interphase (SEI) layer or complex film resistances. $R_{lithium}$ is estimated from the diameter of the semicircle in AC impedance spectra. The largest $|Z_{imag}|$ is obtained at approximately 300 Hz throughout the measurement, which strongly indicates that a time constant of the electrode reaction ($Li \leftrightarrow Li^+ + e^-$) is stable even after 500 h, and hence a side reaction is significantly suppressed. Fig. 1(b) shows the storage time dependences of R_{bulk} and $R_{lithium}$. R_{bulk} was constant throughout the measurement, and alternations of the G3–LiTFSA electrolyte bulk did not occurred. Such a stable time dependence was also observed in $R_{lithium}$, even though a slight increase was found in the initial 200 h. Interfacial stabilities at electrolyte/lithium metal interface are strongly affected by the dissolved anions of lithium salt [19]. It was confirmed from the reduction potential of Li/Li^+ that an interface with low reactivity surface film layer was formed between the lithium metal electrode and the G3–LiTFSA (amide anion) electrolyte due to the wide electrochemical potential limit at negative side under static condition. Fig. 2 shows the temperature dependence of $R_{lithium}$ measured after aged over 500 h at 40 °C. This plot clearly indicates that $R_{lithium}$ follows an Arrhenius-type

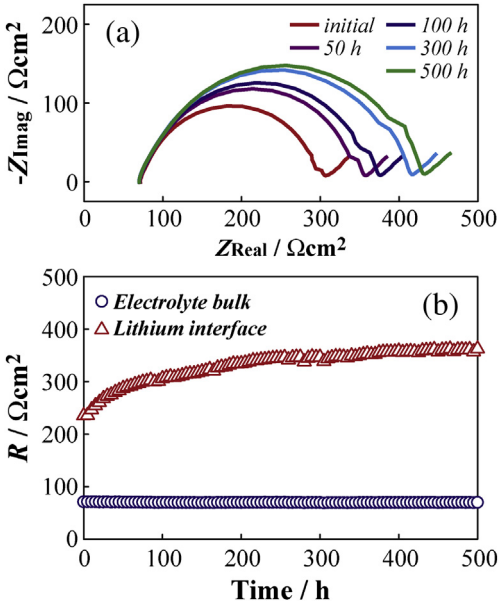

Fig. 1. Storage time dependences of impedance spectrum (a) and electrolyte bulk resistance (R_{bulk}) and interfacial resistance at lithium metal/G3–$LiN(SO_2CF_3)_2$ electrolyte interface ($R_{lithium}$) (b) using [lithium metal|G3–$LiN(SO_2CF_3)_2$ electrolyte|lithium metal] symmetrical cell at 40 °C.

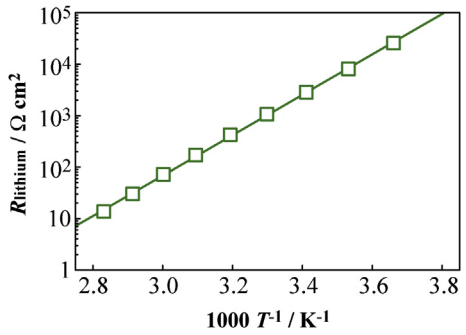

Fig. 2. Temperature dependence of interfacial resistance at lithium metal/G3–LiN(SO_2CF_3)$_2$ electrolyte ($R_{lithium}$) for [lithium metal|G3–LiN(SO_2CF_3)$_2$ electrolyte|lithium metal] symmetrical cell upon heating (0 °C–80 °C) shown as Arrhenius-type plot.

temperature dependence, giving an apparent activation energy (E_a) of 75.2 kJ mol^{-1}. The observed apparent E_a value was close to those reported for other electrolyte systems (organic liquid [20], solid polymer [21], and room-temperature ionic liquid [22]), which means that the same kinds of electrode reaction process occurs on the lithium electrode (Li ↔ $Li^+ + e^-$), even though the frequency factor was different from the other systems.

3.2. 3V-class [$LiFePO_4$|G3–LiTFSA electrolyte|Li metal] cell

On the basis of the results showing the stability of the interface between G3–LiTFSA and the lithium metal electrode under static condition, as mentioned in the previous section, test cells with the working electrodes of $LiFePO_4$ and $LiNi_{1/3}Mn_{1/3}Co_{1/3}O_2$ were prepared for the investigation of the electrochemical performances of positive electrodes. Fig. 3 shows (a) the charge/discharge profiles, (b) the cycle number dependences of the charge and discharge capacities, and (c) the Coulombic efficiencies obtained in a cycle test (voltage range: 2.5–4.0 V, current: *C*/8) of the [$LiFePO_4$ positive electrode|G3–LiTFSA electrolyte|lithium metal negative electrode] cell at 30 °C. Relatively low discharge capacity (approximately 130 mA h g^{-1} per positive electrode) and Coulombic efficiency (approximately 83%) were observed at the first cycle with high polarization between the charge and discharge processes. However, the calculated Coulombic efficiencies found to be close to 100% after two cycles, and stable charge/discharge capacities (over 140 mA h g^{-1} per positive electrode) were obtained within five cycles. The change in the average charge and discharge voltages with the cycle number was extremely little [average charge voltage 3.58 V (1st), 3.50 V (100th), 3.50 V (300th), 3.52 V (500th); average discharge voltage: 3.23 V (1st), 3.34 V (100th), 3.34 V (300th), 3.32 V (500th)], and slight polarization or degradation was observed. Since the increase in polarization by the long cycle (600 cycles) charge/discharge of [$LiFePO_4$ positive electrode|G3–LiTFSA electrolyte|lithium metal negative electrode] cell is very small, it is suggested that the G3–LiTFSA/lithium metal interface are stable under dynamic (charge/discharge) condition as well as the case of static condition mentioned at Section 3.1. Therefore, it is reasonable to conclude that stable electrochemical reactions (positive electrode side: intercalation/deintercalation of lithium, negative electrode side: dissolution/deposition of lithium) take place without any side reactions, which is one of the benefits to use G3–LiTFSA complex as an electrolyte. Note that the cycling for over 600 cycles was attained without significant capacity fading (capacity retention rate: over 99.97%/cycle, calculated from the maximum and minimum discharge capacities). It is inferred that stable long-cycle charge/discharge becomes possible due to the absence of significant oxidative decomposition of electrolyte under the low-voltage operation (in this case, less than 4 V).

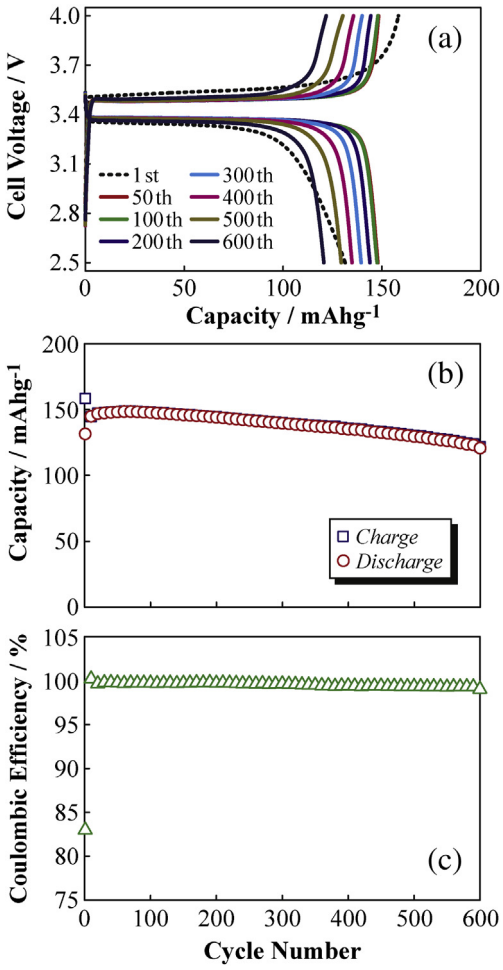

Fig. 3. Charge/discharge profiles of [$LiFePO_4$ positive electrode|G3–LiN(SO_2CF_3)$_2$ electrolyte|lithium metal negative electrode] cell at the 1st, 100th, 200th, 300th, 400th, and 500th cycles (a), cycle number dependences of charge and discharge capacities per positive electrode (b), and Coulombic efficiencies (c) at 30 °C (voltage range: 2.5–4.0 V, current: *C*/8).

3.3. 4V-class [$LiNi_{1/3}Mn_{1/3}Co_{1/3}O_2$|G3–LiTFSA electrolyte|Li metal] cell

It is reasonable to apply G3–LiTFSA to electrolyte for the higher-voltage class positive electrode (<4.0 V), which contributes high energy density lithium secondary batteries. We actually carried out to check the battery performance using $LiCoO_2$ positive electrode [15], and confirmed that the battery worked over 200 cycles. In order to further raise the battery performance, we switch an electrode material to $LiNi_{1/3}Mn_{1/3}Co_{1/3}O_2$ and investigate the long-cycle performance above 4.0 V. Fig. 4(a) shows the charge/discharge profiles obtained in a cycle test (voltage range: 2.7–4.2 V, current: *C*/8) of the [$LiNi_{1/3}Mn_{1/3}Co_{1/3}O_2$ positive electrode|G3–LiTFSA electrolyte|lithium metal negative electrode] cell at 30 °C. A relatively high discharge capacity (approximately 150 mA h g^{-1} per positive electrode) was obtained in the first cycle, which corresponds to approximately 52% of the theoretical capacity of $Li_xNi_{1/3}Mn_{1/3}Co_{1/3}O_2$ (283.7 mA h g^{-1}, $0 < x < 1$), even though first irreversible capacity (1st Coulombic efficiency: 87.5%) was large. Generally, $LiNi_{1/3}Mn_{1/3}Co_{1/3}O_2$ has been reported to have a low initial Coulombic efficiency (approximately 90%, electrolyte: EC/DMC–1 M $LiPF_6$) [23]. The average discharge voltage was 3.74 V and the calculated energy density was approximately 553 W h kg^{-1} at the first cycle. Although polarization increased with the charge/discharge cycle number

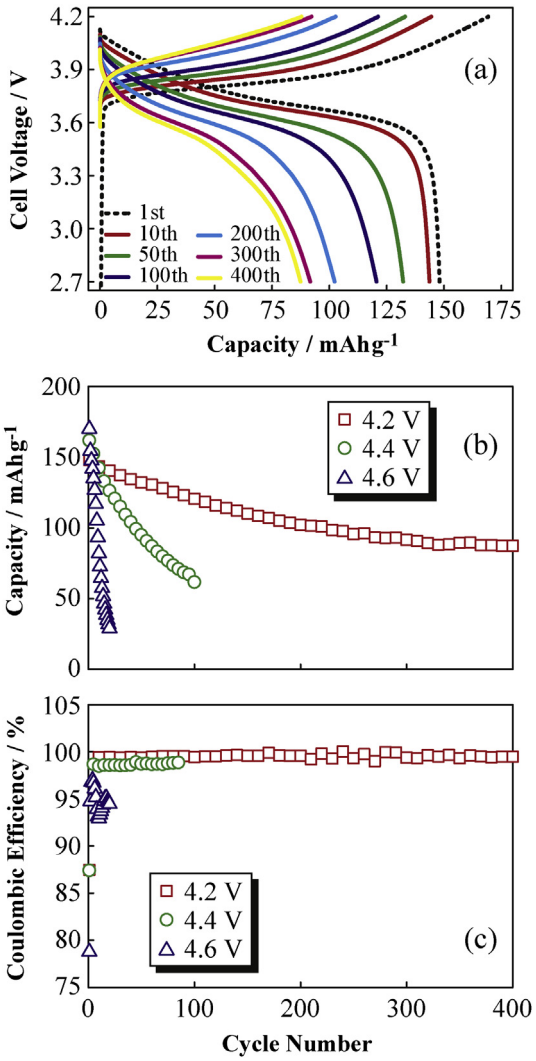

Fig. 4. Charge/discharge profiles of [$LiNi_{1/3}Mn_{1/3}Co_{1/3}O_2$ positive electrode|G3–LiN(SO_2CF_3)$_2$ electrolyte|lithium metal negative electrode] cell at the 1st, 10th, 50th, 100th, 200th, 300th, and 400th cycles (a, voltage range: 2.7–4.2 V, current: *C*/8), cycle number dependences of discharge capacities per positive electrode (b), and Coulombic efficiencies (c) for different upper charge cutoff voltages (4.2 V, 4.4 V, 4.6 V) at 30 °C.

(attributed to the increased resistance of the cells), stable charge/discharge operation continues up to 400 cycles. We have reported the stable charge/discharge operation of a 4V-class $LiCoO_2$ positive electrode after 200 cycles [15], and similar tendency of capacity decreases was confirmed with the both $LiCoO_2$ and $LiNi_{1/3}Mn_{1/3}Co_{1/3}O_2$ cells. The present results demonstrate favorable feature for the long cycle life due to the suitable combination of the highly-oxidation-resistant glyme–lithium salt equimolar complex electrolyte and the $LiNi_{1/3}Mn_{1/3}Co_{1/3}O_2$ positive electrode.

To clarify the upper charge cutoff voltage and cycle properties of the prepared cells, the cycle number dependences of the charge and discharge capacities (b) and Coulombic efficiencies (c) were also plotted by changing upper charge cutoff voltages and are shown in Fig. 4. When the upper charge cutoff voltage was low (4.2 V), sufficient capacity retention was achieved for more than 400 cycles (approximately 60% of the first discharge capacity). However, when the upper charge cutoff voltage is increased, the charge/discharge reversibility became diminished (in particular, 4.6 V), even though the initial discharge capacity increased. This tendency correlates with the previously reported results of oxidative stability using linear sweep voltammetry [14]. A similar tendency for Coulombic efficiency was also observed with increasing upper charge cutoff voltage. Judged from the stable interfacial behavior of the G3–LiTFSA electrolyte/lithium metal electrode, as shown in Figs. 1 (static interface) and 3(a) (under charge/discharge), the most inferable factor causing the decrease of capacity is degradation at the $LiNi_{1/3}Mn_{1/3}Co_{1/3}O_2$ positive electrode/G3–LiTFSA electrolyte interface, owing to instability of positive electrode at high voltage (e.g., release of oxygen). On the other hand, the cell in which the upper charge cutoff voltage was set to 4.2 V exhibited almost 100% Coulombic efficiency; this result is consistent with the slight capacity decrease with increasing charge/discharge cycle number. As was mentioned before, glyme–lithium salt equimolar complex electrolytes have the potential to be used as new electrolyte materials for safe lithium secondary batteries under suitable operation voltage conditions. In particular, molar ratio of glyme and lithium cation at electrode interfaces (both positive and negative electrodes) may shift at the case of charge/discharge. Supposing molar ratio of glyme and lithium cation is important for battery performances (electrode stability), it will be expected that investigation of concentration profile during electrochemical reactions becomes key factors. In near future, we will report the physicochemical properties at the electrochemical interface by using electrochemical quartz microbalance method and charge/discharge behavior of other composition (molar ratio, co-solvent) electrolytes to understand specific nature of the glyme–lithium salt complex electrolytes.

4. Conclusions

To explore the possibility of its practical application to lithium secondary batteries, the electrochemical behavior and battery performance of a glyme (CH_3–O–(C_2H_4O)$_3$–CH_3)–lithium salt (LiN(SO_2CF_3)$_2$) equimolar complex electrolyte were investigated using the lithium metal and two different positive electrode materials ($LiFePO_4$, $LiNi_{1/3}Mn_{1/3}Co_{1/3}O_2$). The electrolyte/lithium metal electrode interface was sufficiently stable for use in lithium secondary batteries, and an apparent activation energy of approximately 75 kJ mol^{-1} was obtained for the reaction Li ↔ $Li^+ + e^-$, which was close to the values reported for other electrolyte systems. Moreover, stable charge/discharge operation (600 cycles) of a 3V-class [$LiFePO_4$ positive electrode|G3–LiN(SO_2CF_3)$_2$ electrolyte|lithium metal negative electrode] cell was achieved due to the high electrochemical stability of the electrolyte and compatibility with the electrode materials (positive and negative). A 4V-class [$LiNi_{1/3}Mn_{1/3}Co_{1/3}O_2$ positive electrode|G3–LiN(SO_2CF_3)$_2$ electrolyte|lithium metal negative electrode] cell exhibited relatively favorable charge/discharge operation (60% of initial discharge capacity after 400 cycles) under suitable voltage conditions (2.7–4.2 V).

Acknowledgments

This work was partially supported by the Advanced Low Carbon Technology Research and Development Program (ALCA) from the Japan Science and Technology Agency (JST), Japan.

References

[1] M. Armand, J.-M. Tarascon, Nature 451 (2008) 652.
[2] A. Nishimoto, K. Agehara, K. Furuya, T. Watanabe, M. Watanabe, Macromolecules 32 (1999) 1541.
[3] S. Matsui, T. Muranaga, H. Higobashi, S. Inoue, T. Sakai, J. Power Sources 97–98 (2001) 772.
[4] S. Seki, Y. Kobayashi, H. Miyashiro, Y. Mita, T. Iwahori, Chem. Mater. 17 (2005) 2041.
[5] F. Mizuno, A. Hayashi, K. Tadanaga, M. Tatsumisago, Adv. Mater. 17 (2005) 918.

[6] N. Kamaya, K. Homma, Y. Yamakawa, M. Hirayama, R. Kanno, M. Yonemura, T. Kamiyama, Y. Kato, S. Hama, K. Kawamoto, A. Mitsui, Nat. Mater. 10 (2011) 682.
[7] H. Sakaebe, H. Matsumoto, Electrochem. Commun. 5 (2003) 594.
[8] H. Nakagawa, S. Izuchi, K. Kuwana, T. Nukuda, Y. Aihara, J. Electrochem. Soc. 150 (2003) A695.
[9] B. Garcia, S. Lavallee, G. Perron, C. Michot, M. Armand, Electrochim. Acta 49 (2004) 4583.
[10] J.-H. Shin, W.A. Henderson, S. Passerini, J. Electrochem. Soc. 152 (2005) A978.
[11] C. Tiyapiboonchaiya, J.M. Pringle, J. Sun, N. Byrne, P.C. Howlett, D.R. MacFarlane, M. Forsyth, Nat. Mater. 3 (2004) 29.
[12] S. Seki, Y. Kobayashi, H. Miyashiro, Y. Ohno, A. Usami, Y. Mita, N. Kihira, M. Watanabe, N. Terada, J. Phys. Chem. B 110 (2006) 10228.
[13] T. Tamura, T. Hachida, K. Yoshida, N. Tachikawa, K. Dokko, M. Watanabe, J. Power Sources 195 (2010) 6095.
[14] T. Tamura, K. Yoshida, T. Hachida, M. Tsuchiya, M. Nakamura, Y. Kazue, N. Tachikawa, K. Dokko, M. Watanabe, Chem. Lett. 39 (2010) 753.
[15] K. Yoshida, M. Nakamura, Y. Kazue, N. Tachikawa, S. Tsuzuki, S. Seki, K. Dokko, M. Watanabe, J. Am. Chem. Soc. 133 (2011) 13121.
[16] K. Yoshida, M. Tsuchiya, N. Tachikawa, K. Dokko, M. Watanabe, J. Electrochem. Soc. 159 (2012) A1005.
[17] N. Tachikawa, K. Yamauchi, E. Takashima, J. Park, K. Dokko, M. Watanabe, Chem. Commun. 47 (2011) 8157.
[18] S. Seki, K. Takei, H. Miyashiro, M. Watanabe, J. Electrochem. Soc. 158 (2011) A769.
[19] K. Kanamura, H. Tamura, S. Shiraishi, Z. Takehara, Electrochim. Acta 40 (1995) 913.
[20] Y. Kobayashi, Y. Mita, S. Seki, Y. Ohno, H. Miyashiro, N. Terada, J. Electrochem. Soc. 154 (2007) A677.
[21] S. Seki, S. Tabata, S. Matsui, M. Watanabe, Electrochim. Acta 50 (2004) 379.
[22] S. Seki, Y. Ohno, Y. Kobayashi, H. Miyashiro, A. Usami, Y. Mita, H. Tokuda, M. Watanabe, K. Hayamizu, S. Tsuzuki, M. Hattori, N. Terada, J. Electrochem. Soc. 154 (2007) A173.
[23] T. Ohzuku, Y. Makimura, Chem. Lett. 30 (2001) 642.